# Nanomedicines for Inflammatory Arthritis: Head-to-Head Comparison of Glucocorticoid-Containing Polymers, Micelles, and Liposomes

Lingdong Quan,[†,◆] Yijia Zhang,[†,◆] Bart J. Crielaard,[‡,¶] Anand Dusad,[†] Subodh M. Lele,[§] Cristianne J. F. Rijcken,[⊥] Josbert M. Metselaar,[∥] Hana Kostková,[#] Tomáš Etrych,[#] Karel Ulbrich,[#] Fabian Kiessling,[▽] Ted R. Mikuls,[⊗,○] Wim E. Hennink,[‡] Gert Storm,[‡,∥] Twan Lammers,[‡,∥,▽,*] and Dong Wang[†,*]

[†]Department of Pharmaceutical Sciences, University of Nebraska Medical Center, Omaha, Nebraska 68198, United States, [‡]Department of Pharmaceutics, Utrecht Institute for Pharmaceutical Sciences, Utrecht University, Universiteitsweg 99, 3584 CG Utrecht, The Netherlands, [§]Department of Pathology and Microbiology, University of Nebraska Medical Center, Omaha, Nebraska 68198, United States, [⊥]Cristal Delivery B.V., Oxfordlaan 55, 6229 EV Maastricht, The Netherlands, [∥]Department of Targeted Therapeutics, MIRA Institute for Biomedical Technology and Technical Medicine, University of Twente, PO Box 217, 7500 AE, Enschede, The Netherlands, [#]Institute of Macromolecular Chemistry AS CR, v.v.i., Heyrovského nám. 2, 162 06 Prague 6, Czech Republic, [▽]Department of Experimental Molecular Imaging, University Clinic and Helmholtz Institute for Biomedical Engineering, RWTH—Aachen University, Pauwelsstrasse 30, 52074 Aachen, Germany, [⊗]Omaha VA Medical Center, 4101 Woolworth Avenue, Omaha, Nebraska 68198, United States, and [○]Department Internal Medicine, Division of Rheumatology, University of Nebraska Medical Center, Omaha, Nebraska 68198, United States. [◆]L. Quan and Y. Zhang contributed equally to this work. [¶]Present address: Department of Pediatrics, Weill Cornell Medical College, 525 East 68th Street, New York, New York 10065, United States.

ABSTRACT As an emerging research direction, nanomedicine has been increasingly utilized to treat inflammatory diseases. In this head-to-head comparison study, four established nanomedicine formulations of dexamethasone, including liposomes (L-Dex), core-cross-linked micelles (M-Dex), slow releasing polymeric prodrugs (P-Dex-slow), and fast releasing polymeric prodrugs (P-Dex-fast), were evaluated in an adjuvant-induced arthritis rat model with an equivalent dose treatment design. It was found that after a single i.v. injection, the formulations with the slower drug release kinetics (*i.e.*, M-Dex and P-Dex-slow) maintained longer duration of therapeutic activity than those with relatively faster drug release kinetics, resulting in better joint protection. This finding will be instructional in the future development and optimization of nanomedicines for the clinical management of rheumatoid arthritis. The outcome of this study also illustrates the value of such head-to-head comparison studies in translational nanomedicine research.
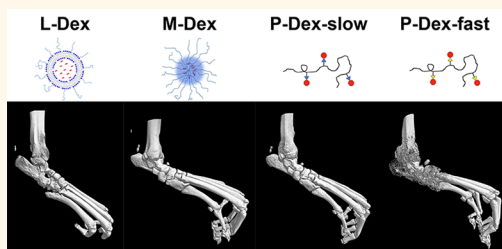
KEYWORDS: nanomedicine · drug targeting · inflammation · rheumatoid arthritis · glucocorticoid · dexamethasone · liposome · micelle · HPMA copolymer

The past few decades have witnessed an exponential growth of nanotechnology-based therapeutic interventions, with many drug delivery platforms, such as water-soluble polymers, polymeric micelles, liposomes, and nanoparticles, being explored to improve disease treatment. As we observe the evolution of the nanomedicine field, improvement of anticancer therapy has undoubtedly been the major driving force. Since cancer still is one of the most devastating human diseases in the developed world, it is not surprising that the majority of nanomedicines developed thus far have aimed to improve current cancer treatment.[1−3]

In recent years, however, nanomedicines have also been increasingly explored for the treatment of inflammatory disorders. Liposomal formulations, for instance, have been developed for the targeted delivery of glucocorticoids (GC) to areas of inflammation, in particular to inflamed joints in the case of rheumatoid arthritis (RA), but also inflammatory lesions in Crohn's disease, colitis, stroke, multiple sclerosis, and atherosclerosis.[4−12] Upon entrapment in ~100 nm-sized PEGylated liposomes, significant improvements in the anti-inflammatory activity of GC have been observed in animal models of all of these diseases.
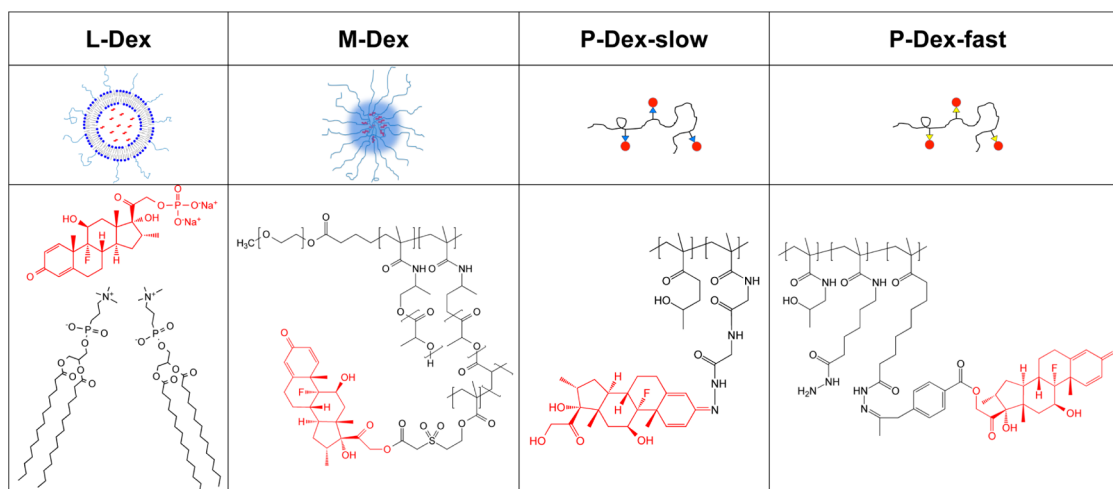
Figure 1. Schematic representation and chemical structures of the four dexamethasone-containing nanomedicine formulations evaluated. L-Dex, long-circulating PEGylated liposome encapsulating dexamethasone phosphate (red) in its aqueous core. M-Dex, dexamethasone-loaded core-cross-linked polymeric micelle. Dexamethasone is covalently entrapped in the hydrophobic core of the polymeric micelle *via* a sulphone ester-containing linker, allowing hydrolytic release of the drug. P-Dex-slow, dexamethasone was covalently conjugated to HPMA copolymer through acid-cleavable hydrazone bond. P-Dex-fast, dexamethasone was covalently conjugated to HPMA polymer through hydrazone benzyl ester bond.

For RA treatment, in particular, an initial clinical trial (ClinicalTrials.gov Identifier: NCT00241982) has confirmed the potential of such inflammation-targeted nanotherapeutic interventions.

Polymeric drug delivery systems have also been shown to be able to selectively target sites of inflammation and to significantly improve the therapeutic efficacy of GC in animal models of inflammatory shock, arthritis, lupus nephritis, and orthopedic implant loosening.[13−21] In addition, the *N*-(2-hydroxypropyl) methacrylamide (HPMA) copolymer-based prodrugs were found to be able to avert some side effects commonly associated with GC when compared to dose-equivalent regimens of the parent drug.[20] The application of liposomes as frontrunner carrier materials for the targeted delivery of GC is a logical one, in view of their clinical track record and their well-established characteristics (*e.g.*, drug loading capacity, biodegradability, safety, *etc.*). Nevertheless, it is also warranted to assume that the use of liposomes may have limitations regarding the control over (prolonged) *in vivo* drug release kinetics. This is due to the fact that drug molecules are entrapped within the liposomal bilayer and might therefore be rapidly released upon the *in vivo* destabilization of lipid bilayers, in particular upon uptake by macrophages.[9] Consequently, it is reasonable to assume that the covalent coupling of drugs to long-circulating polymeric carriers may offer important advantages, if the linker chemistry employed enables optimally "tailored" *in vivo* release kinetics.[13,16,22−25]

Here, we have set out for the first time to directly compare the intensity and duration of therapeutic activity of four previously established and optimized dexamethasone (Dex)-containing nanomedicine formulations[10,17,26,27] (Figure 1) for the treatment of

inflammatory arthritis, using an equidose experimental design (10 mg/kg) and a well-established and clinically relevant rat model of adjuvant-induced arthritis.[28] This direct head-to-head comparison hints toward the use of covalent drug linkages within nanomedicines, enabling sustained release kinetics to achieve long-term disease remission upon a single i.v. injection. This study not only underlines the importance of controlling drug release, but also demonstrates that head-to-head comparisons can render more effective candidate identification and clinical translation of nanomedicines.

RESULTS

***In Vitro* Release of Dexamethasone from Four Different Dex-Containing Nanomedicines.** The *in vitro* drug release kinetics of the four nanomedicine formulations (*i.e.*, liposome-encapsulated Dex (L-Dex), Dex-conjugated core-cross-linked polymeric micelles (M-Dex), slow-releasing HPMA copolymer-dexamethasone prodrug (P-Dex-slow) and fast-releasing HPMA copolymer-dexamethasone prodrug (P-Dex-fast); see Figure 1) were evaluated at pH = 5.0 and 7.4. As shown in Figure 2, in good agreement with previous reports,[16,26] the release of Dex from both HPMA copolymer-dexamethasone conjugates was found to be much faster at acidic pH than at neutral pH. When Dex was conjugated to the HPMA copolymer *via* hydrazone-benzyl ester, it cleaved much faster than Dex conjugated *via* hydrazone bond. By the end of the 14 day follow-up, ∼90% of the Dex from P-Dex-fast was released, while only slightly more than 10% of Dex was released from P-Dex-slow. The release of Dex from the core-cross-linked polymeric micelles was also found to be pH-dependent.[27] At neutral pH, the Dex released at a much faster rate (>17% released by 14 days) than at
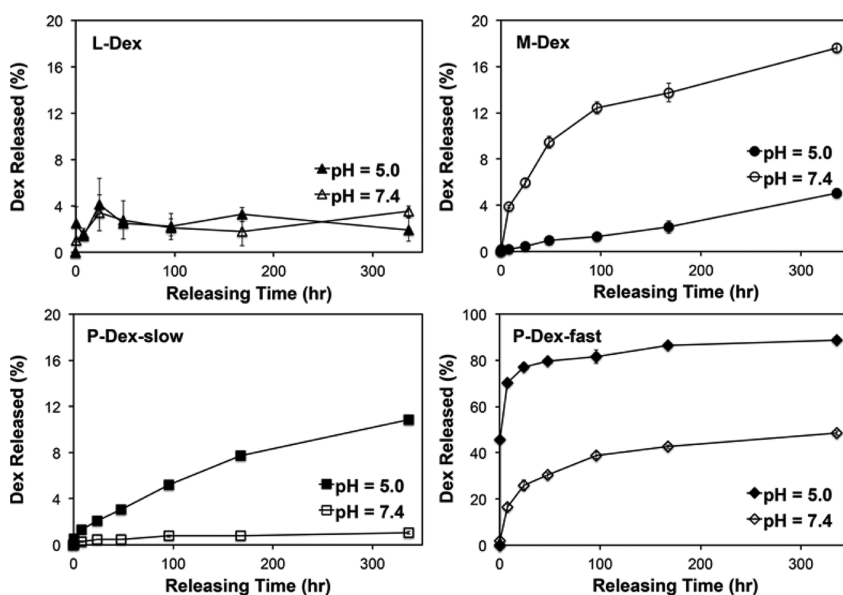
Figure 2. *In vitro* release of dexamethasone from the four nanomedicine formulations at pH = 5.0 and 7.4. The Dex released percentage values are presented as average ± SD.

acidic pH (∼5% released by 14 days). The release of Dex from the liposome formulation was minimal at both acidic and neutral pH. It should be kept in mind in this regard, however, that liposomes rapidly release their contents upon internalization by macrophages.[41]

Preclinical Evaluation of the Four Nanomedicines Formulations in Adjuvant-Induced Arthritis Rats. L-Dex, M-Dex, P-Dex-slow, and P-Dex-fast were then evaluated head-to-head in an adjuvant-induced arthritis (AA) rat model, with free Dex, saline, and healthy untreated rats acting as controls. On day 9 or 10 post arthritis induction, disease activity became apparent with mild swelling and an increase of ankle diameters (Figure 3). On day 15, when the increase in ankle size reached a plateau, a single dose of each of the four Dex-containing nanomedicine formulations was administered i.v. at an equivalent dexamethasone dose (10 mg/kg). For L-Dex, it has been reported that a single dose of 1 mg/kg is sufficient for a complete remission of joint inflammation.[33] For the present equidose study, however, a higher dose of 10 mg/kg Dex was selected, to reveal potential differences in duration of action among the various formulations. For tolerability purposes, an equivalent dose of free Dex had to be divided into four portions, and was administered *via* i.p. injections on four consecutive days (2.5 mg of dexamethasone/kg/day; *i.e.*, within the highest recommended dose range for Dex[34]).

As shown in Figure 3, all treatments, including free Dex, improved the signs of joint inflammation immediately and significantly. The degree of ankle swelling was markedly reduced in all treatment groups during days 15−18, *i.e.*, the first 4 days after treatment. In contrast to the similar pattern of rapid initial response, the duration of the therapeutic benefit resulting from the five treatments was different. For the free Dex group, upon initial suppression, a (re-)flare in joint inflammation was observed immediately upon the cessation of the treatment. A relatively rapid (re-)flare was also observed in the P-Dex-fast group (already at day 6 after i.v. injection). For L-Dex, the effect of treatment lasted longer (until day 10 after i.v. injection). At the dose level evaluated, *i.e.*, 10 mg/kg, P-Dex-slow and M-Dex resulted in the most prolonged suppression of joint inflammation (>30 days). This pronounced improvement in the duration of therapeutic activity of a single injection of P-Dex-slow and M-Dex could be further illustrated by the accumulative disease load (defined as the area under the arthritis score curve[27]) of rats treated with these formulations when compared with all other treatments (Figure 3, $P < 0.0001$, one-way ANOVA). No death was observed throughout the course of the experiment. Regarding mild to moderate toxicity, except for P-Dex-slow, all the other Dex-containing nanomedicines resulted in a certain degree of diarrhea immediately upon treatment. But in all cases, this was rapidly resolved (*i.e.*, within 2−3 days).

Histological Validation. Histological analyses of ankle joint sections were performed at the end of the study (*i.e.*, day 42), to compare bone and cartilage preservation in all treatment groups. As shown in the upper panels in Figure 4, arthritic joints from P-Dex-fast, L-Dex, free Dex, and saline-treated animals all demonstrated cartilage and bone erosion with marked infiltration of mononuclear cells and pannus formation. Joint sections from the L-Dex-treated group showed intermediate inflammatory features. Although the arthritis had started to (re-)flare after an initially very strong anti-inflammatory response, there were only limited cellular infiltrates among animals treated with either P-Dex-slow and M-Dex. There were no obvious
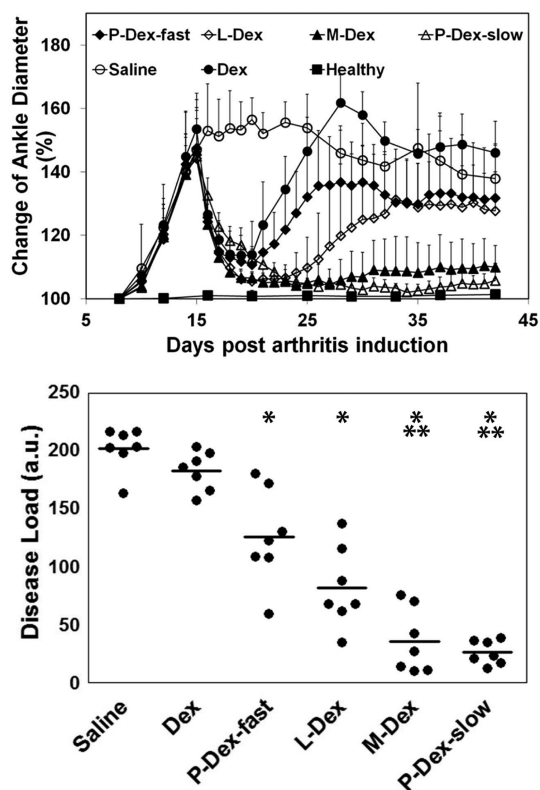
Figure 3. Therapeutic efficacy of Dex-containing nanomedicine treatment in rats with adjuvant-induced arthritis (AA). Top: Change of ankle diameters (%), representing the swelling and disease activity, was determined daily by using a digital caliper. Bottom: The cumulated disease load, defined as the area under the arthritis score curve from treatment (day 15) until the end of the study (day 39), of each individual rat is presented together with the mean of the treatment group as a straight line. The disease load of the animals in each treatment group was significantly different from those in the other groups except for Saline *vs* Dex, P-Dex-fast *vs* L-Dex, M-Dex *vs* P-Dex-slow. *Significantly different from saline and Dex groups. **Significantly different from P-Dex-fast and L-Dex groups.

bone or cartilage erosions, nor any pannus tissue formation observed for these groups. Quantitative scoring of histopathological tissue sections further verified these observations: as shown in the lower panels in Figure 4, the joints from rats treated with either P-Dex-slow or M-Dex presented with the lowest average histology scores (range 0.14−0.29), and values were found to be similar to those observed in healthy controls. The joints of rats treated with L-Dex and P-Dex-fast presented with intermediate histology scores (>3), *i.e.*, significantly higher than those in the P-Dex-slow and M-Dex groups, but lower than the values (>6) found in animals treated with free Dex or saline.

Quantitative Joint Bone Quality Evaluation upon Nanomedicine Treatment. To further assess the potential of the different nanomedicine formulations for preserving joint anatomy and function, mean BMD from the distal tibia to the phalanges of the foot was analyzed at the end of the study (Figure 5). BMD values of the ankle
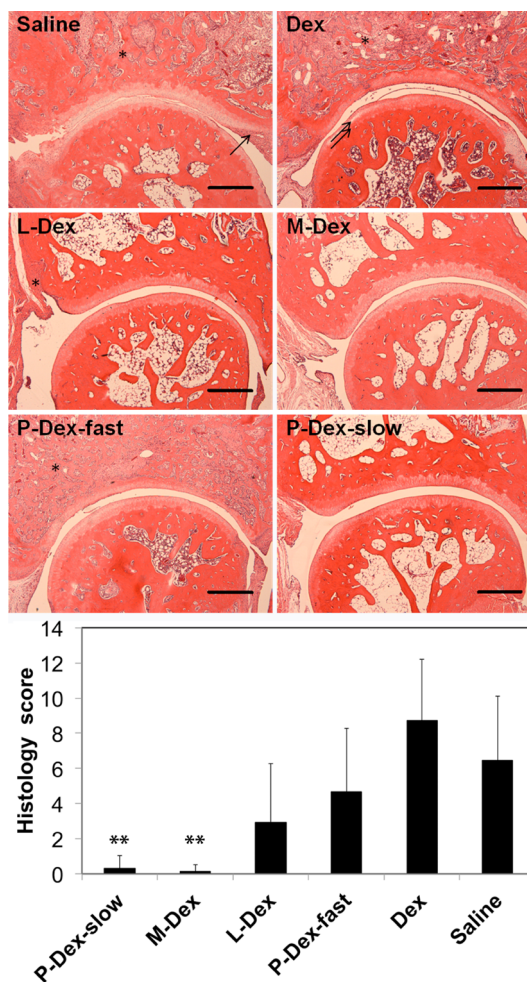

Figure 4. Histological evaluation of the ankle joints nanomedicine-treated AA rats. Top panels: Representative images (40×, H&E staining) of ankle joints. Synovial cell lining hyperplasia, pannus formation (single arrow), bone destruction (*) and cartilage damage (double arrow) are clearly evident in saline, free Dex, P-Dex-fast, and L-Dex treated groups, while the M-Dex and P-Dex-slow treatment efficiently prevented these pathological changes. Bar = 0.5 mm. Bottom panel: P-Dex-slow and M-Dex treated rats showed significantly lower histology scores as compared to free Dex or saline treated rats. **Significantly different from saline and Dex groups.

joints in P-Dex-fast, free Dex, and saline-treated animals were significantly lower than those in the healthy controls ($P < 0.05$). BMD values in the P-Dex-slow and M-Dex treated animals were similar to that of healthy groups, and were significantly higher as compared to those in P-Dex-fast, free Dex, and saline-treated controls (Figure 5). BMD values of L-Dex treated animals tended to be higher than those in P-Dex-fast, free Dex, and saline-treated controls, but lower than those found in P-Dex-slow and M-Dex treated animals. Again, this result may reflect the relatively longer duration of the therapeutic activity of the P-Dex-slow and M-Dex compared to the L-Dex and P-Dex-fast formulations.

The 2D BMD results were supported by 3D micro-CT analyses of the joints. As shown in the reconstructed images in Figure 6, the most severely damaged joints

were found in the saline-treated group, with almost the entire distal tibia being eroded. All of the nanomedicine formulations of Dex as well as equivalent dose of free Dex offered a protection to the joints. The level of joint damage generally conformed to the following order: saline > Dex > P-Dex-fast > L-Dex, followed by very minor bone surface erosion observed for M-Dex- and P-Dex-slow-treated joints. The quantitative analysis of the hind paw calcaneus micro-CT data convincingly showed that P-Dex-slow and M-Dex treatment

most efficiently preserved the bone volume fraction (BV/TV), trabecular thickness (Tb.Th), trabecular number (Tb.N) and mean polar moment of inertia (MMI), with values similar to those observed for healthy controls, and significantly better than those observed for free Dex-treated and saline-treated animals ($P < 0.01$; Table 1).

DISCUSSION

As a class of very potent and fast-acting anti-inflammatory drugs with proven disease-modifying effects, GCs have well-known and readily recognized side effects,[35,36] primarily due to their ubiquitous biodistribution. Several different nanomedicine formulations, including liposomes (L-Dex), water-soluble polymers (P-Dex-fast and P-Dex-slow), and polymeric micelles (M-Dex), have been successfully developed to modify the biodistribution of GCs, aiming to improve therapeutic efficacy and safety.[9,10,15−17,26,27,37]

In this head-to-head comparison study, we found that both M-Dex and P-Dex-slow treatments yielded sustained anti-inflammatory activity providing complete preservation of the joint structure of the AA rats. Though fast and intense in their action, the therapeutic effects of L-Dex and P-Dex-fast treatment appeared more short-lived and therefore offered only partial protection to the joint anatomy, as the observation
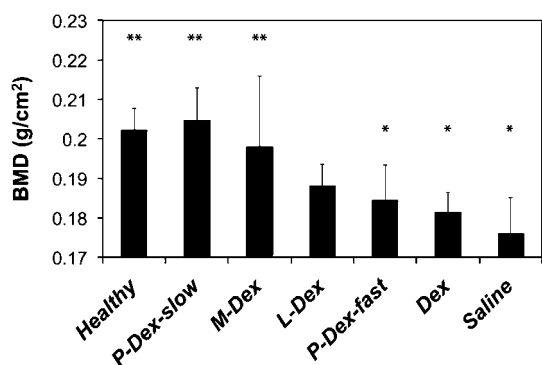

Figure 5. End point bone mineral density (BMD) of the ankle joints for all the animal groups. BMD was evaluated with peripheral dual energy X-ray absorptiometry (pDEXA). *Significantly different from healthy control group. **Significantly different from saline and Dex groups.
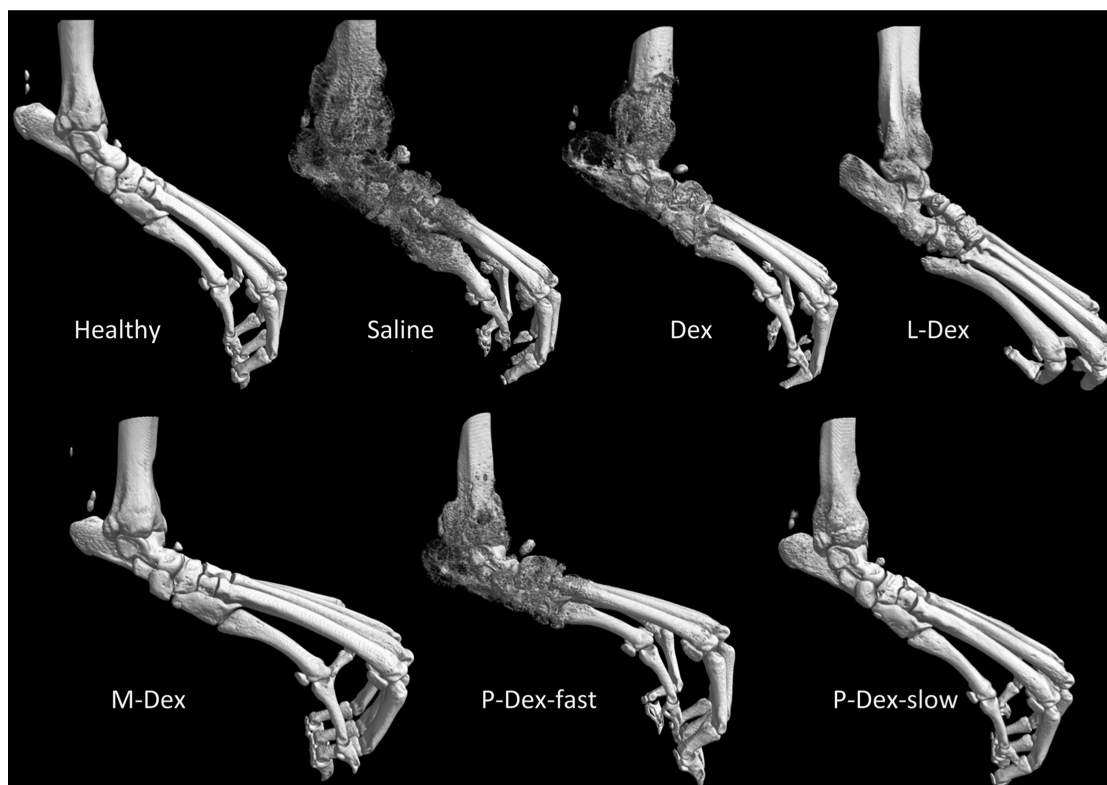
Figure 6. Representative microcomputed tomography (micro-CT) images of the ankle joints of Dex-containing nanomedicine-treated AA rats. Micro-CT scans showed significant bone erosions in the saline, Dex, or P-Dex-fast groups. Prominent bone erosions were evident on the calcaneus bone and extended to the metatarsals. Minor erosions were seen in these areas within the ankle joints of L-Dex treated rats. P-Dex-slow and M-Dex presented with an impressive reduction of ankle joint bone erosions, where bone was well-preserved and appeared to be similar to that found in healthy rats.

TABLE 1. Ankle Joint Bone Histomorphometric Parameters from Adjuvant-Induced Arthritis (AA) Rats Treated with Four Different Nanomedicine Formulations of Dexamethasone (Obtained from Analyses of the Micro-CT Data)[a]

	BV/TV (%)	Tb.Pf	SMI	Tb.Th	Tb.N	MMI
saline	8.35	37.80	2.54	0.07	0.93	0.007
Dex	9.99	28.65	2.49	0.08	1.01	0.009
P-Dex-fast	29.32[b]	12.20	1.63	0.10	2.56[b]	0.026[b]
L-Dex	32.67[b]	2.36	1.52[b]	0.11	2.94[b]	0.030[b]
M-Dex	37.99[b]	−1.43[b]	1.25[b]	0.12[b]	3.22[b]	0.034[b]
P-Dex-slow	39.76[b]	−1.78[b]	1.15[b]	0.12[b]	3.40[b]	0.036[b]
healthy	38.35[b]	−0.04[b]	1.28[b]	0.11[b]	3.48[b]	0.036[b]

[a] BV/TV = Bone volume fraction or bone volume density; Tb.Pf = trabecular bone pattern factor; SMI = structure model index; Tb.Th = trabecular thickness; Tb.N = trabecular number; MMI = mean polar moment of inertia. [b] Significantly different as compared to the saline and free Dex groups.

time point was relatively late and the disease started to progress again. For these two formulations, more frequent administration at a lower dosing level may achieve treatment outcomes similar to those with slower activation profiles (M-Dex and P-Dex-slow).

According to the proposed mechanism of action of these nanomedicines,[9,17,21,27] carrier-specific features such as nature, size, and structure, which likely affect their circulation half-life, extravasation, penetration, internalization, and/or drug release kinetics, will have direct impact on the therapeutic efficacy and the durability of response for the nanomedicine tested. In this study, all treatments contained the same antirheumatic drug, dexamethasone, with exactly the same dosing level, and all were tested in the same animal model of inflammatory arthritis. The first structural parameter that differentiates the four nanomedicines is their size. For P-Dex-fast and P-Dex-slow, these conjugates share similar average hydrodynamic radius (R_H = 5.9 and 5.0 nm, respectively). As for M-Dex and L-Dex, their average diameters are ∼53 nm and ∼96 nm, respectively. The head-to-head study design allowed us to quickly rule out the possibility of having nanomedicine size as the major contributing factor for their different efficacy in this particular animal model of inflammatory arthritis. As the treatment data reveals (Figures 3−6), P-Dex-fast and P-Dex-slow, while having a similar hydrodynamic radius, provided the shortest and the longest anti-inflammatory activity duration, respectively. On the other hand, though M-Dex and P-Dex-slow have very different sizes, they both very effectively ameliorated the synovitis for a very long duration (>30 days) and preserved the joint anatomy and structure. We speculate that the vascular permeability in the tested AA rats' synovia is so high that it permits extravasation of all four tested nanomedicine formulations, leading to a similar extravasation rate. For subclinical RA (with mild inflammatory conditions), however, the extent of vascular permeability may limit the rate of extravasation with the increase of nanomedicine size.[38,39]

Further assessment of the results from this study suggests that the Dex release kinetics of the nanomedicine formulations, rather than their size, may be the major parameter contributing to their different therapeutic activity duration. As reported previously, Dex in P-Dex-fast was conjugated to the polymer backbone through a hydrazone-benzyl ester.[26] It hydrolyzes at a much faster rate than the vinyl bond-stabilized hydrazone linker in P-Dex-slow (Figure 2). Because of the acid labile nature of the linker chemistry, the main Dex releasing sites for P-Dex-slow and P-Dex-fast are the endosomal/lysosomal compartments or inflammation associated acidosis pathology. In M-Dex, Dex was conjugated to the cross-linked core *via* a sulfone ester bond, which hydrolyzes faster at physiological pH than in acidic environments[27] (Figure 2). Such linker chemistry design permits Dex release from M-Dex to proceed at both intracellular compartments and extracellular space.[40] Though L-Dex was found to have a very slow release rate as compared to the other three formulations in standard releasing buffers (Figure 2), their *in vivo* drug release rates are expected to reverse. Our previous studies have shown that upon extravasation into the arthritic joint, liposomal formulations interact with macrophage-like synoviocytes, resulting in the rapid release of the encapsulated drug following lysosomal degradation.[9,41] The extensive phagocytosis of L-Dex within inflamed tissue exposes the macrophage-like synoviocytes to high intracellular concentrations of Dex, which may explain its both rapid and robust anti-inflammatory effect. As macrophage-triggered drug release from L-Dex is much faster[41] than drug release from P-Dex-slow[16] and M-Dex,[27] its anti-inflammatory effects are expected to have a relatively shorter duration than P-Dex-slow and M-Dex (Figure 3). It is important to note that what was encapsulated in the liposomes is free Dex (dexamethasone phosphate disodium), a water-soluble prodrug of Dex. Because of its rapid *in vivo* conversion to dexamethasone,[42] the onset of its therapeutic action will not be affected.

To consider this finding in a bigger picture, it is important to point out that because of the equidose study design, L-Dex treatment is likely "overdosed" at the level of 10 mg/kg. It is already effective (albeit with shorter therapeutic activity duration) at a much lower dose (1 mg/kg), at which neither P-Dex-slow nor M-Dex show efficacy.[16,27,33] Similarly, it might be possible that some of these formulations can even be safely administered at a higher dose (*i.e.*, the maximum tolerated dose; MTD), potentially leading to an even longer suppression of disease parameters upon a single i.v. injection. These possibilities will be investigated in more detail in future studies.

Considering the potential clinical translation of the nanomedicines under study, one may question which formulation is preferred: a formulation effective in a low dose and a shorter duration of action, or a

formulation administered at higher doses but with a longer duration of action? Prior to answering these questions, dose—response, pharmacokinetics, as well as detailed safety studies will need to be carried out to clearly outline the therapeutic potential of the various formulations. In addition, regarding the best choice for a particular clinical application, other factors such as clinical needs (*e.g.*, bridging therapy *vs* long-term prescription), patient compliance (all nanomedicine evaluated must be given as injections), ease and costs of manufacturing, biocompatibility, pharmacokinetics, and targeting efficiency also need to be taken into consideration.

CONCLUSION

In this head-to-head comparison study, we have evaluated the therapeutic activity duration of four established nanomedicine formulations of dexamethasone in a clinically relevant animal model of inflammatory arthritis. It was found that a longer duration of action is achieved when Dex is covalently conjugated to (polymeric) carrier materials using linker chemistry permitting sustained drug release and prolonged systemic and/or local drug activity. This finding is instructional in the future development and optimization of nanomedicines for the clinical management of rheumatoid arthritis. Furthermore, the study presented in this paper also suggests that as opposed to many common beliefs, nanomedicines may find greater success in inflammatory diseases than in cancer, because of more prominent, consistent and homogeneous passive targeting to the lesion. Though never performed in the past, we believe such head-to-head comparison study is essential for the future nanomedicine design, optimization, and clinical translation.

MATERIALS AND METHODS

Preparation of Dexamethasone Encapsulating Long-Circulating Liposomes. L-Dex was prepared by lipid film-hydration method.[9,10] Briefly, DPPC (Lipoid GmbH, Germany), PEG2000-DSPE (Lipoid), and cholesterol (Sigma Aldrich, Germany) were dissolved in a 1.85:0.15:1 molar ratio in 5—10 mL of ethanol. A lipid film was formed in a round-bottom flask *via* rotary evaporation (Buchi, Switzerland) and further dried under a nitrogen flow. The lipid film was then hydrated with a 100 mg/mL solution of dexamethasone phosphate disodium (free Dex, BUFA, The Netherlands) in reversed osmosis purified water to form liposomes. The size and polydispersity of the liposomes were reduced by repeated extrusion of the dispersion through two polycarbonate filters with varying pore sizes (Whatman, USA) mounted in an LIPEX extruder (Northern Lipids Inc., Canada). Unencapsulated free Dex was removed by dialysis against PBS at 4 °C for 48 h. The dexamethasone concentration in the liposomal dispersion (6.5 mg/mL) was measured, upon extraction of the aqueous phase,[29] by ultraperformance liquid chromatography (UPLC) (Waters) equipped with an Acquity UPLC BEH C18 column, using acetonitrile/water (1/3) with 0.1% TFA as eluent. Particle diameter (96 nm) and polydispersity index (PDI, 0.14) of extruded dispersions were determined by dynamic light scattering (DLS) using a Nano-ZS instrument (ZEN3600, Malvern).

Preparation of Dexamethasone-Conjugated Core-Cross-Linked Polymeric Micelles. M-Dex was prepared as described previously.[27] Briefly, a polymerizable prodrug of dexamethasone (DMSL3)[27] was encapsulated in the hydrophobic core of polymeric micelles, using the rapid heating method.[30,31] One volume of DMSL3 in ethanol was added to nine volumes of an ice-cold ammonium acetate buffered (pH = 5) solution of poly(ethylene glycol)-*b*-poly(*N*-(2-hydroxypropyl)methacrylamide lactate) (PEG-*b*-pHPMAmLacn) copolymer with 14% methacrylation, KPS (Merck, USA) and TEMED (Sigma Aldrich, Germany). The final concentration of polymer, KPS, TEMED and DMSL3 (Dex equivalent) was 20, 1.35, 3, and 2 mg/mL, respectively. Subsequently, by rapid heating to 50 °C while stirring vigorously for 1 min, polymeric micelles were formed. The micelles were covalently stabilized by radical polymerization of the methacrylated polymer side chains present in the micellar core in a N$_2$-atmosphere for 1 h at RT, and as a result of copolymerization of DMSL3 during cross-linking, Dex-conjugated core-cross-linked polymeric micelles were obtained. Finally, the micelles were filtered with a 0.2 μm filter to remove aggregated nonencapsulated drug. The amount of dexamethasone conjugated within the micelles (1.6 mg/mL, which corresponded to an encapsulation efficiency of 80%) was determined by UPLC upon hydrolysis of the ester bonds at pH 9.4, which was considered complete when a plateau in the dexamethasone concentration was reached. The diameter of the polymeric micelles, as determined by dynamic light scattering, is approximately 53 nm, with a PDI of 0.04.

Preparation of Two HPMA Copolymer-Dexamethasone Conjugates. P-Dex-slow was synthesized and characterized as described previously.[16] Briefly, *N*-(2-hydroxypropyl)methacrylamide (HPMA) and acid-cleavable *N*-methacryloylglycylglycylgycyl hydrazonyl dexamethasone (MA-Gly-Gly-NHN=Dex) were copolymerized by RAFT polymerization at 50 °C for 2 days, with 2,2′-azobisisobutyronitrile (AIBN) as initiator and *S,S′*-bis(α,α'-dimethyl-α''-acetic acid)-trithiocarbonate as RAFT agent. The resulting polymer was first purified on a LH-20 column to remove the unreacted low molecular weight compounds and then dialyzed. The molecular weight cutoff of the dialysis tubing was 25 kDa. The polymer solution was lyophilized to obtain the final P-Dex-slow. The hydrodynamic radii (R_H) of the polymer carriers in a phosphate buffer (0.01 g/mL; pH 7.4, 0.1 M with 0.05 M NaCl) were measured with a Nano-ZS instrument (ZEN3600, Malvern). The intensity of scattered light was detected at θ = 173° using a laser at 632.8 nm. For the evaluation of dynamic light scattering data, the DTS (Nano) program was used. The value was the mean of at least five independent measurements. The R_H (5.0 nm) of P-Dex-slow was found to be rather stable over 2 days of measurements, with M_w = 49.4 kDa and M_n = 27.7 kDa. The amount of Dex conjugated in the P-Dex-slow was determined as 9.6 wt % (fully hydrolyzed, analyzed with HPLC).

P-Dex-fast was synthesized and characterized as reported previously.[26] As the first step, 4-(2-oxopropyl)benzoic acid ester of Dex (Dex-OPB) was synthesized by reacting the hydroxyl group on C21 of Dex with 4-(2-oxopropyl)benzoic acid. 6-Methacrylamidohexanohydrazide (Ma-ah-NHNH$_2$) was then prepared. The copolymerization of HPMA and Ma-ah-NHNH$_2$ was done in methanol at 60 °C for 17 h with AIBN as initiator. As a polymer precursor, the resulting copolymer poly(HPMA-co-Ma-ah-NHNH$_2$) was then used in a polymer analogous reaction with Dex-OPB to obtain the final product of P-Dex-fast. The Dex content in P-Dex-fast was 8.5 wt %. Because of the difference in linker chemistry, P-Dex-fast has a much higher release rate than P-Dex-slow.[16,26] The initial R_H of P-Dex-fast was 5.9 nm, with M_w = 33.3 kDa and M_n = 18.2 kDa. Over the course of 2 days incubation in PBS, however, a gradual increase of scattered light intensity suggests the formation of aggregates due to quick Dex release.

Analysis of Dexamethasone Release from the Four Nanomedicine Formulations. The release of free Dex and/or Dex esters, from soluble polymer conjugates and from micelles were investigated by incubation of the conjugates in phosphate buffers at pH 5.0 and 7.4 (0.1 M phosphate buffer with 0.05 M NaCl) at 37 °C. The concentration of the conjugate in stock solution was equivalent to 2.5×10^{-4} M Dex. At predetermined time

intervals, 200 μL of the solution was withdrawn, extracted with chloroform (0.8 mL), and then analyzed with an HPLC analyzer (Shimadzu, Japan), using a reverse-phase column Chromolith Performance RP-18e (100 × 4.6, eluent water—acetonitrile with acetonitrile gradient 0—100 vol %, flow rate 0.5 mL/min) with UV detection at 230 nm.

For Dex phosphate release from liposomes (2.5 × 10^{-4} M, Dex concentration), the liposomes were incubated in phosphate buffers at pH 5.0 and 7.4 (0.1 M phosphate buffer with 0.05 M NaCl) at 37 °C. At predetermined time intervals, 500 μL of the solution was placed onto PD-10 column (eluent PBS buffer), and the fraction containing low-molecular weight molecules (including Dex phosphate) was collected and freeze-dried. The Dex phosphate was extracted from the lyophilized sample into methanol and analyzed with HPLC as mentioned above.

Evaluation of Dexamethasone Formulations in Adjuvant-Induced Arthritis Rats. Male Lewis rats (175—200 g) were obtained from Charles River Laboratories, Inc. (Wilmington, MA, USA) and allowed to acclimate for at least 1 week. Arthritis was induced by subcutaneous injection of 1 mg of *Mycobacterium tuberculosis* H37Ra and 5 mg of *N,N*-dioctadecyl-*N′*,*N′*-bis(2-hydroxyethyl)-1,3-propanediamine mixed in 100 μL of paraffin oil at the base of the rats' tail.[14] On day 15, rats (7/group) with established arthritis were treated i.v. with saline, and 10 mg/kg Dex equivalent of L-Dex, M-Dex, P-Dex-fast, and P-Dex-slow. An equivalent dose of free Dex was divided into four aliquots (2.5 mg of dexamethasone/kg) and administered i.p. to another group of AA rats on days 15—18. Six healthy Lewis rats were included as a control group. From day 8, clinical symptoms of joint inflammation were assessed, and the medial to lateral ankle diameter was determined using a digital caliper, as a measure of inflammatory swelling. Arthritis flare of the latest group among four treatment groups was set as the experimental end point, at which time the animals were euthanized with hind limbs isolated for bone mineral density (BMD) and histology evaluations. Cumulative disease load was defined as the area under the arthritis score curve from the start of treatment (day 15) until the end of the study. BMD was measured from the distal tibia to the phalanges of the paw using a pDEXA Sabre X-ray bone densitometer (Norland Medical System, Inc., Fort Atkinson, WI, USA). All animal experiments were performed using a protocol approved by the University of Nebraska Medical Center Institutional Care and Use Committee in accordance with *Principles of Laboratory Animal Care* (National Institutes of Health publication 85—23, revised in 1985).

Microcomputed Tomography Analysis of Joints. Microarchitectural parameters of the ankle joints were evaluated as described previously,[32] using a Skyscan 1172 micro-CT system (Skyscan, Kontich, Belgium). Micro-CT scanning parameters were voltage, 70 kV; current, 142 μA; exposure time, 1400 ms; resolution, 13.1 μm; and aluminum filter (0.5 mm). 3D images were reconstructed using CT-Vox and CT-Vol software (Skyscan), to produce a visual representation of the results. To quantitatively compare the four treatments, the hind paw calcaneus was identified as the anatomical site for micro-CT analysis. The morphometric parameters of subchondral trabecular bone, such as bone volume (BV, mm^3), bone volume fraction (BV/TV, %), trabecular thickness (Tb.Th, μm), trabecular separation (Tb.Sp, μm), and trabecular number (Tb.N, 1/mm), were calculated (software CTAn, Skyscan).

Histological Analysis. Isolated hind limbs were fixed with formalin and decalcified. Once decalcification was complete, specimens were transferred to ammonia solution to neutralize acids and left in specimens for 30 min and then rinsed in water for 24 h. Thin sections (5 μm) were cut approximately 200 μm apart and were H&E stained. The joints were histologically graded by a trained pathologist (SML), using a scoring system as previously described.[17] Each histopathologic feature was graded as follows: synovial cell lining hyperplasia (0—2); pannus formation (0—3); mononuclear cell infiltration (0—3); polymorphonuclear leukocytes infiltration in periarticular soft tissue (0—3); cellular infiltration and bone erosion at distal tibia (0—3); and cellular infiltration of cartilage (0—2). The score for every histopathologic feature was summed for each animal.

Statistics. Values are presented as average ± standard deviation. One-way analysis of variance (ANOVA) was performed followed by a *post hoc* test (Bonferroni's test) for multiple comparisons. A value of $P < 0.05$ was considered statistically significant.

Conflict of Interest: The authors declare the following competing financial interest(s): JMM is an employee and shareholder of Enceladus Pharmaceuticals, a company developing i.v. liposomal corticosteroid products. CJFR is employee and shareholder of Crystal Delivery B.V., a company developing innovative nanomedicines based on its proprietary CriPec nanoparticle platform.

REFERENCES AND NOTES

1. Juliano, R. Nanomedicine: Is The Wave Cresting? *Nat Rev. Drug Discovery* **2013**, *12*, 171–172.
2. Venditto, V. J.; Szoka, F. C., Jr. Cancer Nanomedicines: So Many Papers And So Few Drugs!. *Adv. Drug Delivery Rev.* **2013**, *65*, 80–88.
3. Lammers, T. SMART Drug Delivery Systems: Back To The Future *Vs.* Clinical Reality. *Int. J. Pharm.* **2013**, *454*, 527–529.
4. Awasthi, V. D.; Goins, B.; Klipper, R.; Phillips, W. T. Accumulation Of PEG-Liposomes In The Inflamed Colon Of Rats: Potential For Therapeutic And Diagnostic Targeting Of Inflammatory Bowel Diseases. *J. Drug Targeting* **2002**, *10*, 419–427.
5. Crielaard, B. J.; Lammers, T.; Morgan, M. E.; Chaabane, L.; Carboni, S.; Greco, B.; Zaratin, P.; Kraneveld, A. D.; Storm, G. Macrophages And Liposomes In Inflammatory Disease: Friends Or Foes? *Int J. Pharm.* **2011**, *416*, 499–506.
6. Hofkens, W.; Schelbergen, R.; Storm, G.; van den Berg, W. B.; van Lent, P. L. Liposomal Targeting Of Prednisolone Phosphate To Synovial Lining Macrophages During Experimental Arthritis Inhibits M1 Activation But Does Not Favor M2 Differentiation. *PLoS One* **2013**, *8*, e54016.
7. Hofkens, W.; van den Hoven, J. M.; Pesman, G. J.; Nabbe, K. C.; Sweep, F. C.; Storm, G.; van den Berg, W. B.; van Lent, P. L. Safety Of Glucocorticoids Can Be Improved By Lower Yet Still Effective Dosages Of Liposomal Steroid Formulations In Murine Antigen-Induced Arthritis: Comparison Of Prednisolone With Budesonide. *Int. J. Pharm.* **2011**, *416*, 493–498.
8. Lobatto, M. E.; Fayad, Z. A.; Silvera, S.; Vucic, E.; Calcagno, C.; Mani, V.; Dickson, S. D.; Nicolay, K.; Banciu, M.; Schiffelers, R. M.; *et al.* Multimodal Clinical Imaging To Longitudinally Assess A Nanomedical Anti-Inflammatory Treatment In Experimental Atherosclerosis. *Mol. Pharmaceutics* **2010**, *7*, 2020–2029.
9. Metselaar, J. M.; van den Berg, W. B.; Holthuysen, A. E.; Wauben, M. H.; Storm, G.; van Lent, P. L. Liposomal Targeting Of Glucocorticoids To Synovial Lining Cells Strongly Increases Therapeutic Benefit In Collagen Type II Arthritis. *Ann. Rheum. Dis.* **2004**, *63*, 348–353.
10. Metselaar, J. M.; Wauben, M. H.; Wagenaar-Hilbers, J. P.; Boerman, O. C.; Storm, G. Complete Remission Of Experimental Arthritis By Joint Targeting Of Glucocorticoids With Long-Circulating Liposomes. *Arthritis Rheum.* **2003**, *48*, 2059–2066.
11. Schmidt, J.; Metselaar, J. M.; Wauben, M. H.; Toyka, K. V.; Storm, G.; Gold, R. Drug Targeting By Long-Circulating Liposomal Glucocorticosteroids Increases Therapeutic Efficacy In A Model Of Multiple Sclerosis. *Brain* **2003**, *126*, 1895–1904.

12. Tiebosch, I. A.; Crielaard, B. J.; Bouts, M. J.; Zwartbol, R.; Salas-Perdomo, A.; Lammers, T.; Planas, A. M.; Storm, G.; Dijkhuizen, R. M. Combined Treatment With Recombinant Tissue Plasminogen Activator And Dexamethasone Phosphate-Containing Liposomes Improves Neurological Outcome And Restricts Lesion Progression After Embolic Stroke In Rats. *J. Neurochem.* **2012**, *123* (Suppl 2), 65–74.

13. Timofeevski, S. L.; Panarin, E. F.; Vinogradov, O. L.; Nezhentsev, M. V. Anti-Inflammatory And Antishock Water-Soluble Polyesters Of Glucocorticoids With Low Level Systemic Toxicity. *Pharm. Res.* **1996**, *13*, 476–480.

14. Wang, D.; Miller, S. C.; Sima, M.; Parker, D.; Buswell, H.; Goodrich, K. C.; Kopečková, P.; Kopeček, J. The Arthrotropism Of Macromolecules In Adjuvant-Induced Arthritis Rat Model: A Preliminary Study. *Pharm. Res.* **2004**, *21*, 1741–1749.

15. Wang, D.; Miller, S. C.; Liu, X. M.; Anderson, B.; Wang, X. S.; Goldring, S. R. Novel Dexamethasone-HPMA Copolymer Conjugate And Its Potential Application In Treatment Of Rheumatoid Arthritis. *Arthritis Res. Ther.* **2007**, *9*, R2.

16. Liu, X. M.; Quan, L. D.; Tian, J.; Alnouti, Y.; Fu, K.; Thiele, G. M.; Wang, D. Synthesis And Evaluation Of A Well-Defined HPMA Copolymer-Dexamethasone Conjugate For Effective Treatment Of Rheumatoid Arthritis. *Pharm. Res.* **2008**, *25*, 2910–2919.

17. Quan, L. D.; Purdue, P. E.; Liu, X. M.; Boska, M. D.; Lele, S. M.; Thiele, G. M.; Mikuls, T. R.; Dou, H.; Goldring, S. R.; Wang, D. Development Of A Macromolecular Prodrug For The Treatment Of Inflammatory Arthritis: Mechanisms Involved In Arthrotropism And Sustained Therapeutic Efficacy. *Arthritis Res. Ther.* **2010**, *12*, R170.

18. Liu, X. M.; Miller, S. C.; Wang, D. Beyond Oncology—Application Of HPMA Copolymers In Non-Cancerous Diseases. *Adv. Drug Delivery Rev.* **2010**, *62*, 258–271.

19. Ren, K.; Purdue, P. E.; Burton, L.; Quan, L. D.; Fehringer, E. V.; Thiele, G. M.; Goldring, S. R.; Wang, D. Early Detection And Treatment Of Wear Particle-Induced Inflammation And Bone Loss In A Mouse Calvarial Osteolysis Model Using HPMA Copolymer Conjugates. *Mol. Pharmaceutics* **2011**, *8*, 1043–1051.

20. Yuan, F.; Nelson, R. K.; Tabor, D. E.; Zhang, Y.; Akhter, M. P.; Gould, K. A.; Wang, D. Dexamethasone Prodrug Treatment Prevents Nephritis In Lupus-Prone (NZB X NZW)F1 Mice Without Causing Systemic Side Effects. *Arthritis Rheum.* **2012**, *64*, 4029–4039.

21. Yuan, F.; Quan, L. D.; Cui, L.; Goldring, S. R.; Wang, D. Development Of Macromolecular Prodrug For Rheumatoid Arthritis. *Adv. Drug Delivery Rev.* **2012**, *64*, 1205–1219.

22. Chytil, P.; Etrych, T.; Konak, C.; Šírova, M.; Mrkvan, T.; Říhová, B.; Ulbrich, K. Properties Of HPMA Copolymer-Doxorubicin Conjugates With pH-Controlled Activation: Effect Of Polymer Chain Modification. *J. Controlled Release* **2006**, *115*, 26–36.

23. Etrych, T.; Šírova, M.; Starovoytova, L.; Říhová, B.; Ulbrich, K. HPMA Copolymer Conjugates Of Paclitaxel And Docetaxel With pH-Controlled Drug Release. *Mol. Pharmaceutics* **2010**, *7*, 1015–1026.

24. Lammers, T.; Ulbrich, K. HPMA Copolymers: 30 Years Of Advances. *Adv. Drug Delivery Rev.* **2010**, *62*, 119–121.

25. Talelli, M.; Iman, M.; Varkouhi, A. K.; Rijcken, C. J.; Schiffelers, R. M.; Etrych, T.; Ulbrich, K.; van Nostrum, C. F.; Lammers, T.; Storm, G.; *et al.* Core-Crosslinked Polymeric Micelles With Controlled Release Of Covalently Entrapped Doxorubicin. *Biomaterials* **2010**, *31*, 7797–7804.

26. Krakovicova, H.; Etrych, T.; Ulbrich, K. HPMA-based polymer conjugates with drug combination. *Eur. J. Pharm. Sci.* **2009**, *37*, 405–412.

27. Crielaard, B. J.; Rijcken, C. J.; Quan, L.; van der Wal, S.; Altintas, I.; van der Pot, M.; Kruijtzer, J. A.; Liskamp, R. M.; Schiffelers, R. M.; van Nostrum, C. F.; *et al.* Glucocorticoid-Loaded Core-Cross-Linked Polymeric Micelles With Tailorable Release Kinetics For Targeted Therapy Of Rheumatoid Arthritis. *Angew. Chem., Int. Ed. Engl.* **2012**, *51*, 7254–7258.

28. Bendele, A. Animal Models Of Rheumatoid Arthritis. *J. Musculoskeletal Neuronal Interact.* **2001**, *1*, 377–385.

29. Bligh, E. G.; Dyer, W. J. A Rapid Method Of Total Lipid Extraction And Purification. *Can. J. Biochem. Physiol.* **1959**, *37*, 911–917.

30. Rijcken, C. J.; Veldhuis, T. F.; Ramzi, A.; Meeldijk, J. D.; van Nostrum, C. F.; Hennink, W. E. Novel Fast Degradable Thermosensitive Polymeric Micelles Based On PEG-Block-Poly(N-(2-Hydroxyethyl)Methacrylamide-Oligolactates). *Biomacromolecules* **2005**, *6*, 2343–2351.

31. Rijcken, C. J.; Snel, C. J.; Schiffelers, R. M.; van Nostrum, C. F.; Hennink, W. E. Hydrolysable Core-Crosslinked Thermosensitive Polymeric Micelles: Synthesis, Characterisation And *In Vivo* Studies. *Biomaterials* **2007**, *28*, 5581–5593.

32. Manolides, A. S.; Cullen, D. M.; Akhter, M. P. Effects Of Glucocorticoid Treatment On Bone Strength. *J. Bone Miner. Metab.* **2010**, *28*, 532–539.

33. van den Hoven, J. M.; Hofkens, W.; Wauben, M. H.; Wagenaar-Hilbers, J. P.; Beijnen, J. H.; Nuijen, B.; Metselaar, J. M.; Storm, G. Optimizing The Therapeutic Index Of Liposomal Glucocorticoids In Experimental Arthritis. *Int. J. Pharm.* **2011**, *416*, 471–477.

34. Carpenter, J. W.; Mashima, T. Y.; Rupiper, D. J. *Exotic Animal Formulary*, 2nd ed.; W.B. Saunders: Philadelphia, PA, 2001; Vol. xiv, p 423.

35. Barnes, P. J.; Adcock, I. M. Glucocorticoid Resistance In Inflammatory Diseases. *Lancet* **2009**, *373*, 1905–1917.

36. Galon, J.; Franchimont, D.; Hiroi, N.; Frey, G.; Boettner, A.; Ehrhart-Bornstein, M.; O'Shea, J. J.; Chrousos, G. P.; Bornstein, S. R. Gene Profiling Reveals Unknown Enhancing And Suppressive Actions Of Glucocorticoids On Immune Cells. *FASEB J.* **2002**, *16*, 61–71.

37. Quan, L. D.; Yuan, F.; Liu, X. M.; Huang, J. G.; Alnouti, Y.; Wang, D. Pharmacokinetic And Biodistribution Studies Of N-(2-Hydroxypropyl)Methacrylamide Copolymer-Dexamethasone Conjugates In Adjuvant-Induced Arthritis Rat Model. *Mol. Pharmaceutics* **2010**, *7*, 1041–1049.

38. Yuan, F.; Dellian, M.; Fukumura, D.; Leunig, M.; Berk, D. A.; Torchilin, V. P.; Jain, R. K. Vascular Permeability In A Human Tumor Xenograft: Molecular Size Dependence And Cutoff Size. *Cancer Res.* **1995**, *55*, 3752–3756.

39. Yuan, F.; Leunig, M.; Huang, S. K.; Berk, D. A.; Papahadjopoulos, D.; Jain, R. K. Microvascular Permeability And Interstitial Penetration Of Sterically Stabilized (Stealth) Liposomes In A Human Tumor Xenograft. *Cancer Res.* **1994**, *54*, 3352–3356.

40. Coimbra, M.; Rijcken, C. J.; Stigter, M.; Hennink, W. E.; Storm, G.; Schiffelers, R. M. Antitumor Efficacy Of Dexamethasone-Loaded Core-Crosslinked Polymeric Micelles. *J. Controlled Release* **2012**, *163*, 361–367.

41. Cittadino, E.; Ferraretto, M.; Torres, E.; Maiocchi, A.; Crielaard, B. J.; Lammers, T.; Storm, G.; Aime, S.; Terreno, E. MRI Evaluation Of The Antitumor Activity Of Paramagnetic Liposomes Loaded With Prednisolone Phosphate. *Eur. J. Pharm. Sci.* **2012**, *45*, 436–441.

42. Rohdewald, P.; Mollmann, H.; Barth, J.; Rehder, J.; Derendorf, H. Pharmacokinetics Of Dexamethasone And Its Phosphate Ester. *Biopharm. Drug Dispos.* **1987**, *8*, 205–212.